Feasibility of Micro-Multilayer Multifunctional Electrical Insulation (MMEI) System for High Voltage Applications

Euy-Sik Eugene Shin
Universities Space Research Association (USRA)
NASA Glenn Research Center
Cleveland, OH, USA
euy-sik.e.shin@nasa.gov

***Abstract*—The newly patented micro-multilayer multifunctional electrical insulation (MMEI) system was developed for future electric aircraft applications which critically require lightweight but high voltage (HV), high temperature, and corona or partial discharge (PD) resistant insulation. During the initial development stages, the concept and practicability of the MMEI system were successfully validated with its exceptionally high dielectric breakdown voltages. The multilayer structures were optimized in terms of material type, individual layer thickness, and overall layer configuration along with potential mechanisms identified for its superior performance. Subsequently, scalability, manufacturability, and commercial applicability of the MMEI system were demonstrated with the 1 meter long, 3-phase HV, high power (HP) bus bar prototypes. Two prototypes, one with the conventional SOA insulation system including Mica sheet and the other with an optimized MMEI, were designed, fabricated, and tested successfully. Both prototypes passed both HiPot and PD tests up to the highest test voltage available, 15 kV_{AC}, although the latter showed a slight increase in PD activities at 12.5 kV. However, the prototype with MMEI was 15% lighter or 12% thinner than the other one. Current efforts to significantly enhance the PD resistance of the MMEI system by employing semiconductive shielding layers, which can be also multifunctional, e.g., electromagnetic interference shielding, moisture blocking, heat dissipation, for various HV applications are also discussed in this paper.**

Keywords—novel electrical insulation, high voltage, lightweight, multilayer, multifunctionality, semiconductive shield

I. Introduction and Background

The increasing need for clean energy is pushing technology development in the aeronautics and space sector toward electrified propulsion systems [1,2]. Major challenges in designing electric propulsion are to meet the high power (HP) requirements and to reduce the overall system weight [2,3]. Conventionally, this would require larger currents and thus larger conductors which would result in huge weight and volume increases although heavy mechanical and pneumatic machines would be removed. Employing high voltage (HV) and/or high frequency (HF) systems is a viable solution, but then that would require much thicker insulation, again contributing to significant weight gain. Furthermore, the insulation should be resistant to partial discharge (PD) for high-altitude operation as well as high thermal-electrical-mechanical stresses. Therefore, development of a lightweight but HV, HF, high temperature, and PD resistant electrical insulation system was one of the most critical prerequisites for the successful electrified propulsion system.

The novel concept of the micro-multilayer multifunctional electrical insulation (MMEI) system was developed over its effectiveness and flexibility with regard to design-process-performance relations to meet the aforementioned requirements [1,2,4,5]. Later, a US patent [6] was granted as its concept and feasibility were successfully validated with its exceptionally high dielectric breakdown voltages (V_B) over the state-of-the-art (SOA) polymer insulations regardless of test conditions when they were optimized in terms of materials, individual layer thickness, and layer configuration. Multifunctionality was another major thrust for the MMEI development obviously for its structural concept and design ability. Other important multifunctionalities needed for such applications besides those mentioned above included moisture barrier, electro-magnetic interference (EMI) shielding, mechanical durability, thermal management or heat dissipation. However, adding functional layers caused negative impact on the overall V_B of MMEI and it was not only material dependent but also structure dependent, thus, more systematic, and careful design and optimizations are required to incorporate multifunctionalities into MMEI. It is also worth noting that even though the initial data indicated that the MMEI structures were more effective at high voltages above 20 kV based on the standard V_B, their development was still relevant to the lower voltage applications since tests have shown that insulation life is inversely proportional to the AC operating frequency. Furthermore, when frequency, temperature, and voltage stress derating factors are all combined, insulation with a rating of 10,000 V for the 1-min test may be reduced to less than a few hundred volts in operational application [7].

For more accurate and practical assessment of the MMEI system, V_B of various SOA insulation materials and structures were systematically determined in terms of thickness and test environment and compared with performance of the newly optimized MMEI structures, Fig. 1 [5]. The Cirlex® PI laminates and the most well-known SOA aircraft insulation system, e.g., Teflon-Kapton-Teflon (TKT: note that samples tested were not

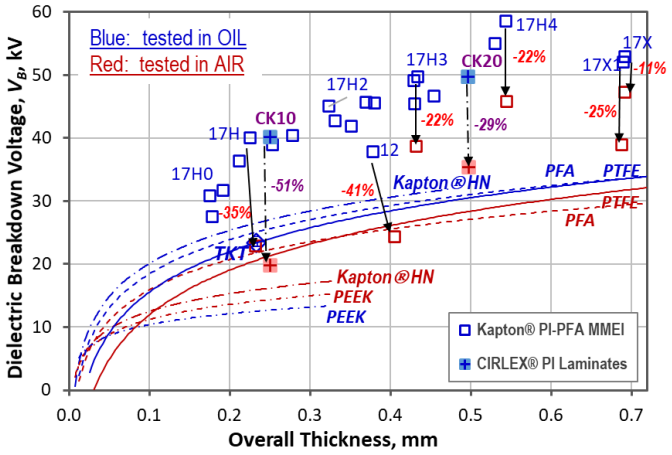

Fig. 1. Overall dielectric performance of various MMEI structures to date compared to the SOA commercial insulation materials including TKT and Cirlex® laminates, CK10 and CK20.

from a commercial product but fabricated in the lab based on [4,5]) were also included for direct comparison. Overall, the MMEI structures, particularly the better-performing configurations, e.g., [1*HN/1*PFA]n/1*HN, outperformed all others regardless of overall sample thickness or test medium. The V_B drop when tested in air, $\Delta V_{B,\ AIR\text{-}to\text{-}OIL}$, was the smallest in pure polymer insulations, but MMEI showed smaller changes than the Cirlex® laminates. The effects of current type, AC vs DC, on V_B of the SOA insulation materials and MMEI structures were also assessed with a few representative samples in oil. In all cases, $V_{B,DC}$ was significantly higher than $V_{B,AC}$ and again MMEI outperformed other insulations.

At the same time, potential mechanisms responsible for the enhanced MMEI performance were suggested [4] and validated experimentally via 3-dimensional dielectric breakdown damage zone (DZ) analysis by serial polishing and subsequent high resolution micrographing in the RoboMet 3D automated system (UES, Inc., Dayton, OH) [5]. The MMEI structures with higher V_B, typically consisted of thinner individual layers, induced a significantly more torturous path for HV current flow through the insulation layers, Fig. 2, compared to those of thicker layers, Fig. 3, or other insulations tested. Moreover, formation or propagation of damage such as defects/voids in the MMEI structures was effectively suppressed with decreasing the individual layer thickness, typically less than 1 mil/25.4 µm.

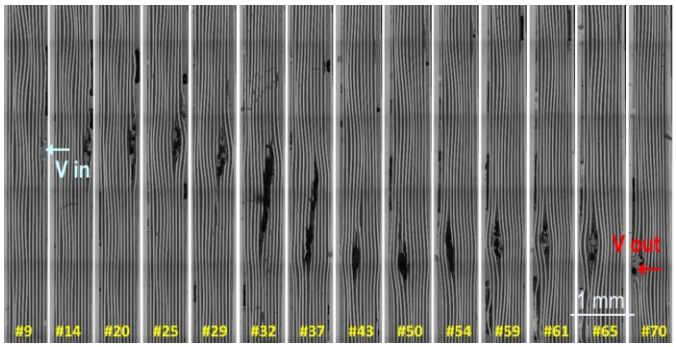

Fig. 2. Sequence of representative cross-sectional micrographs of the damage and failure zone in 17H4 MMEI ([1*HN/1*PFA]$_{10}$/1*HN) tested in air. (Note: the sequential number of the selected cross-sections are listed at bottom Typical cross-sectional interval was ~ 50-100 µm)

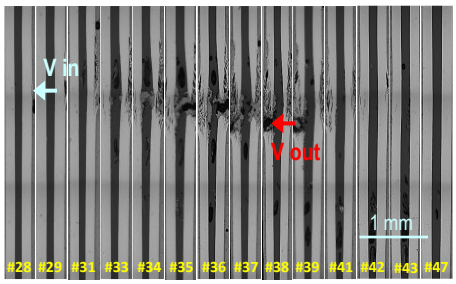

Fig. 3. Same as Fig. 2 but for 5*HN/5*PFA/5*HN

Additionally, this 3-D DZ analysis confirmed that the size of DZ was directly proportional to V_B in general.

Since then, efforts were focused to develop PD-resistant MMEI structures and full-scale demonstrations for scalability, manufacturability, and commercial applicability of the MMEI system. Progresses in such efforts are updated in this paper.

II. Experimental

The materials used or compared in MMEI development, MMEI fabrication methods including prototypes, and property characterization techniques, e.g., V_B, utilized in this work were described previously [1,4,5]. The typical layup convention for the MMEI configurations used throughout this paper is, for example, [1*HN/1*PFA]n/1*HN where the asterisk mark indicated thickness in mils (1/1000 of inch or 0.0254 mm), the capital letters stand for name or type of material, the slash for next layer, and the subscripted number after bracket is the number of repeated layup sequence within the bracket.

A. Materials

For the purpose of comparison with MMEI structures, a commercial alternative multilayer candidate, CIRLEX® Kapton® HN laminate sheet, 10 mil and 20 mil thick, designated as CK10 and CK20, respectively, which was developed by Fralock with the proprietary adhesiveless lamination process was also evaluated in this study.

Various constituent materials used to develop the multi-semiconducting layer (MSL) shields via a solution casting process are listed below:

- 3M™ Dyneon™ PFA 6900GZ aqueous PFA dispersion (3M, Advanced Materials Division): 50wt% solid, 235 nm average particle size (APS), 7wt% polyether-based emulsifier in distilled water; 310°C melting temperature
- Carbon Black: (i) ACM1333864 (ALFA Chemistry, www.alfa-chemistry.com), spherical particles with 150 nm APS; Specific surface area (SSA) >700 m²/g; purity ≥95%; electrical resistivity of 0.30 Ω.cm (CB1), (ii) Ketjenblack EC600-JD, electro-conductive (MSE supplies, https://www.msesupplies.com/), Spherical particles with 34 nm APS; BTE SSA = 1270 m²/g (CB2)
- Graphene Powder (MSE supplies), multi-layer graphene particles with <10 µm APS prepared by thermal exfoliation reduction; SSA = 400-550 m²/g (GP)
- Dispersant for CB dispersion: Marasperse CBOs-4 a highly modified sodium lignosulfonate based dispersant (Borregaard, Norway)

B. Fabrications

MSL shields to enhance partial discharge resistance of MMEI system were initially fabricated by solution casting of aqueous PFA dispersion dispersed with the conductive fillers for a subscale feasibility demonstration. Conventional extrusion or coextrusion can be used for scale-up and commercialization in future. The step-by-step procedures developed and optimized were as follows: 1) Disperse conductive filler(s) into distilled water with dispersant→ 2) mixed via ball-milling with Borosilicate beads in Resodyn Acoustic Mixer (LabRAM II) followed by an optimized mixing condition→ 3) mixed both the filler dispersion and PFA dispersion in LabRAM II followed by an optimized mixing condition to form PFA-conductive filler nanocomposite, namely PFAn dispersion→ 4) applied thin layer of PFAn onto clean polymer insulation film, e.g., PEEK→ 5) dried at temperatures below 90°C/194°F→ 6) stacked PFAn coated polymer films based on a predetermined MSL layer configurations→ 7) compression-molded the stacks at an air-circulated oven preheated to 350°C/662°F for 60 min.

III. Results and Discussion

A. Full-scale Demonstrations

The efforts to demonstrate scalability, manufacturability, and commercial applicability of the MMEI system were made with full-scale prototypes of the representative electrical components for the future electric aircrafts, such as bus bar and power cable [2,4,5]. Development of bus bar prototypes in collaboration with the Mersen of Rochester, New York, specialized in HV bus bar manufacturing was based specifically on 1 meter long, 3 phase targeting to 10 MW power at 20 kV. Two prototypes were designed, fabricated, and tested successfully: one with the conventional SOA insulation system, assembled by the conventional lamination process, and the other with an optimized MMEI, assembled by the vacuum bagging and autoclaving process. The two-prototype approach employed was to achieve more practical and meaningful performance assessment. The SOA insulation materials consisted of PTFE, corona resistant Kapton®100CR, Mica sheet, and silicone or epoxy adhesives for bonding. The down-selected MMEI was 17X having the high V_B of 48 kV in air and further optimized for the PFA-conductor bonding integrity, i.e., Conductor/1*PFA /$[1*PFA/1*HN]_{10}$/$[1*PFA/1*CR]_2$/2*PEEK/0.3*HN. Both prototypes were then clamped particularly to withstand the 8.0 Grms random vibrations specified as Category V aircraft.

The bus bar was tested according to ASTM D149-20, Fig. 4. Both prototypes passed HiPot dielectric breakdown test, up to the highest test voltage available, 15 kV_{AC}, and by meeting the limit of the leakage current, 0.5 mA. Both also passed the PD test, but the prototype with MMEI showed a slight increase in PD activities at 12.5 kV. Mica is known to be the most PD resistant material but it may not be applicable to power cables due to its rigidity, thus additional efforts to enhance PD resistance of MMEI are under way, which is discussed in the last section of this paper. In any case, the prototype with MMEI was 15 % lighter or 12 % thinner than the other with Mica. The results were consistent and acceptable with regards to both manufacturability and performance, especially in that the primary focus of MMEI development was to enhance dielectric strength with reduced thickness. This full-scale demonstration

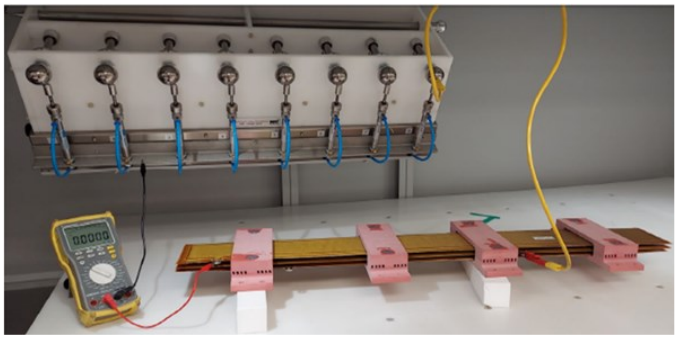

Fig. 4. Standard testing of full-scale 3-phase bus bar prototype.

with the HV bus bar prototypes validated the MMEI system for various HV applications, particularly for future electric aircraft applications.

The prototype development for the power cable was also under way. As published elsewhere [1,4], a flat pod cable consisting of six identical conductors, which were arranged horizontally and capable of carrying 0.25 MW at 15 kV or higher (rated to 40 kV), was designed by the GORE. The first prototype employed GORE's proprietary PTFE-PTFE composite insulation and a corona resistant PTFE jacket, rated to -80 ºC ~ >260 ºC, was completed and being evaluated at GRC and the center for high performance power electronics (CHPPE), Ohio State University (OSU). For the second prototype, similar efforts as the bus bar prototype development described above are being made to manufacture 1-m long cable sections via a batch process of one-step autoclave lamination with the 17X MMEI system. Manufacturability validation of MMEI into a cable form, which involves equipment design and process development with the assistance of industrial cable manufactures is also initiated under the project.

B. PD Behavior of Insulation Materials and Correlation with Leakage Current (LC)

As a part of the efforts to improve PD resistance of MMEI system, PD behavior of various insulation materials was assessed as a function of thickness extensively and systematically in collaboration with CHPPEOSU. The PD inception voltage and extinction voltage (PDIV/PDEV) were determined under 60 Hz AC at two different air pressures, 760 torr/1 atm and 100 torr/0.13 atm (at 48,000 ft altitude) using the custom-designed Cone (2 mm dia.)-to-Plate Electrode setup instrumented with high frequency current transducer PD sensor and Techimp PD BASE acquisition system. As shown in Fig. 5, PDIV was strongly dependent on sample thickness and test pressure regardless of material type. Note that both semi-crystalline polymers performed better than others including Cirlex® laminates and Kapton® PI materials at the atmospheric pressure but at the reduced pressure of 100 torr, PDIV of all samples not only dropped significantly but also fell into similar values/trendline regardless of material type or structures, indicating challenges in developing HV insulation for high altitude applications. Similarly, for both pressures, PDEV showed almost identical behavior as PDIV except that their values were consistently lower, ~ 80-95% of PDIV values, regardless of material type or thickness.

The PD threshold conditions were then compared with LC

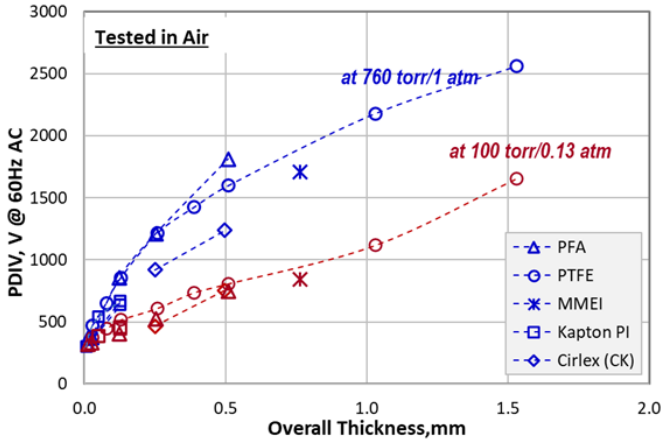

Fig. 5. Partial discharge inception voltage (PDIV) of various insulation materials against sample thickness.

that was directly measured during V_B test [4]. PD and LC were expected to be compatible due to the similar nature and potential mechanisms of LC as reported in literature [8]. The LC was well-defined as a pass-through current proportional to the applied voltage, more prominently under AC, that a dielectric can sustain without leading to runaway currents as a result of dielectric breakdown. It is related to the dielectric material not being a perfect insulator and having some non-zero conductivity, thus, it can be relatable to PD potentials. In general, the lower the LC, the better the insulation. Fig. 6 shows the PDIV-LC correlations at various applied voltages of 2, 5, and 15 kV, respectively. Clearly, PDIV was monotonically related to LC per applied voltage, best-fit with a power trendline, but more importantly it was independent of material type, i.e., confirmed their structural nature. Thus, with these correlations, PD performance of any insulation materials can be estimated by LC which is much simpler and easier to determine during V_B measurement. As expected, PVED-LC correlations also followed the same trends at slightly lower voltage values.

In addition, based on the nature of LC, it could be used to assess thermal stability of insulation materials. As an example, LC of 5*PFA increased considerably after being exposed at 350 °C even for a short time, but no visible changes from any of Kapton® PI films after such thermal exposure. This behavior was consistent with the changes in V_B reported previously [1].

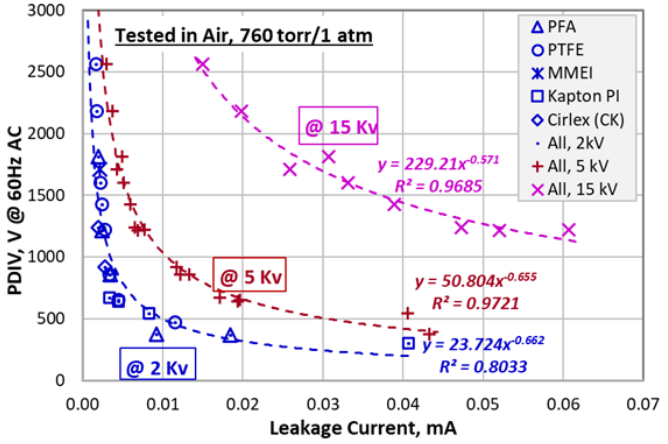

Fig. 6. PDIV-LC relations at various applied voltages regardless of insulation material types.

That is, the Kapton® PI films did not undergo any thermal-induced molecular structural changes or degradation, thus no changes in LC or have better thermal stability than PFA.

C. PD-resistant MMEI

Recently, a major effort was initiated to significantly enhance the PD resistance of the MMEI structures for HV applications by incorporating semiconductive shielding layers, as the typical industry standard and based on well-documented theories and experimental results in literature [9-14]. By taking the advantages of multilayering thin insulation materials again, a so-called multi-semiconducting layer (MSL), as a subset of MMEI which also combines various multifunctionalities as described in Fig. 7, has been designed and evaluated. The MSL structures will be implemented as both conductor shield and insulation shield on both sides of MMEI. The optimum MSL layer configuration developed based on the initial trials in terms of processibility and multifunctionality was 0.3*HN/0.5*PFA /[t*PFAn/0.5*PEEK/t*PFAn]$_2$/t*PFAn/0.5*PEEK/0.3*HN, where PFAn is the semiconductive nanocomposite filled with conductive fillers with a thickness t, i.e., CB or/and GP. With the configuration, the effects of CB type, loading rate, or hybridization with secondary filler (e.g., GP) on fabricability, conductivity percolation threshold, microstructure, and mechanical properties, e.g., flexibility etc. were investigated and thus, to down select the best PFAn compositions, TABLE I. It was suggested that smaller CB particles with higher specific surface area possibly requires much smaller loading than larger CB particles for the required conductivity. It was also suggested that GP has a lower percolation threshold than most CBs and delivers a super conductivity of 8000 S/m or greater since it is highly reduced (C ⩾98 wt%). In most cases, PFAn layers by the brushing application were typically 12.7 – 25.4 µm (0.5 – 1 mil) thick and uniform without blistering or mud-cracking especially for the solutions with lower filler content, less than 10 wt%, Fig. 8. Loading rates of the conductive fillers were verified primarily by the char yield from the thermogravimetric analysis (TGA) at 600 °C where PFA matrix was completely decomposed. Furthermore, the energy-dispersive X-ray spectroscopy (EDS-SEM) dispersion analysis showed that CB fillers were reasonably well-dispersed but more importantly partially to fully connected or formed chain structure, Fig. 9, as one of main electrical percolation mechanism as described in detail elsewhere [11]. Overall, PFAn layers in most MSL coupons were consistent with target compositions and layer thicknesses despite of some scattering, TABLE I. The MSL coupons were then evaluated systematically in terms of various

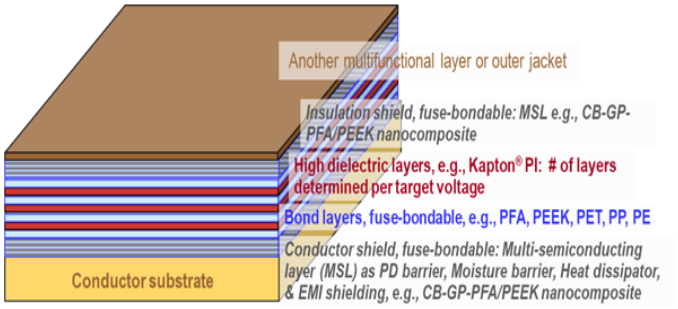

Fig. 7. Updated design concept of future MMEI structures. Note that CB stands for carbon black, GP for Graphene powder, and PI, PFA, PEEK, PET, PP, PE for various polymers.

TABLE I. OVERALL TEST MATRIX FOR MSL OPTIMIZATION

	PFAn layers			PFAn layers		Thickness, mil		
Coupon	Loading, wt%			TGA Char yield		Overall	PFAn, All	
ID	CB1	CB2	GP	Avg, wt%	SD	Avg	Avg	SD
MSL3	20			18.5	4.3	5.00	2.40	0.21
MSL4	20			18.5	4.3	5.00	1.90	0.19
MSL5	30			25.4	6.6	4.65	2.05	0.15
MSL6	10			11.0	4.1	4.80	2.20	0.18
MSL7		3		3.2	1.1	5.53	2.93	0.32
MSL8		5		6.0	3.3	5.34	2.74	0.31
MSL9		10		16.4	3.2	7.00	4.40	0.79
MSL10		20		24.8	5.2	8.90	6.30	0.44
MSL11		2	1	4.6	2.4	7.14	4.54	0.79
MSL12		2	0.5	3.6	0.5	5.78	2.68	0.31
MSL13		2	0.2	4.1	2.0	5.58	2.98	0.25
MSL14	1	1	0.2	3.8	2.8	5.31	2.71	0.38

target properties such as semi-conductivity via in-plane resistance (R)/resistivity(ρ) as a function of temperature up to 300 °C, thermal stability of ρ, thru-thickness V_B and LC, thru-thickness thermal conductivity; processibility; microstructures, e.g., connectivity and uniformity; and structural integrity, e.g., bonding integrity and flexibility. In most case, ρ at room temperature was ranged between 10 to 900 Ω·cm except MSL6 and 13 which had ρ > 20 kΩ·cm, and thermally stable up to 300 °C except MSL5. It was reported [10] that ρ of semiconductive polymer composite shields for high-voltage direct current (HVDC) cable is required to be less than 1,000 Ω·cm. Based on the overall test results including fair to good processability, connectivity, uniformity, and bonding integrity; and reasonable V_B of 7.4kV in air, good thermal conductivity of 0.55 W/m, and low LC, the best composition down selected was 2 wt% CB2 plus 0.5 wt% GP in the balance of PFA which was used for the MSL12 coupon.

With the selected nanocomposite composition, the MSL layer configuration will be further optimized, especially for scaling up before being implemented into MMEI structures. The final modified MMEI structures with the optimized MSL shielding layers will be evaluated for their in-service performances, particularly PDIV/PDEV and EMI shielding efficiency followed by the aforementioned full-scale prototype validations.

IV. SUMMARY AND CONCLUSIONS

The newly developed MMEI system was further optimized and validated with outstanding dielectric performance and associated mechanisms in terms of DZ-failure path-layer dimension relations. The scalability, manufacturability, and commercial applicability of the MMEI system were then

Fig. 8. Typical cross-section from MSL6 coupon.

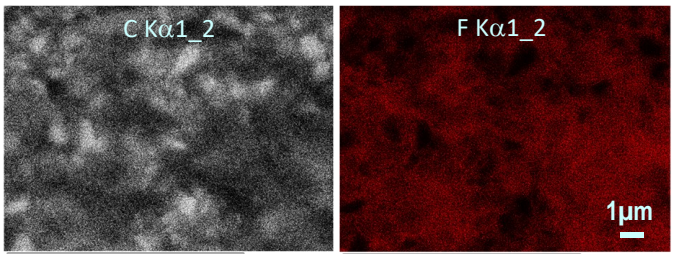

Fig. 9. Typical EDS 2-D mapping images of CB particles (left: C from CB filler in while, right F from PFA matrix in red) in 20wt% CB1-PFA nanocomposites, MSL4.

demonstrated with full-scale bus bar prototypes successfully. Since then, a major effort of significantly enhancing PD resistance of the MMEI structures by incorporating semiconductive shielding layers was initiated. The so-called multi-semiconducting layer (MSL) consisting of thin semiconductive nanocomposite layers and functional polymer insulation films, as a subset of MMEI which also combines various multifunctionalities, was designed and evaluated. To date, its optimum layer configuration, the best nanocomposite composition in terms of conductive filler loading rates, and optimum process conditions and procedures were determined for the full-scale prototype demonstrations of the representative electrical components. In addition, the unique and practical PDIV/PDEV-LC correlations were identified from various SOA insulation materials and structures including MMEI which can be used to gauge PD resistance of the modified MMEI structures or newly developed insulation materials.

ACKNOWLEDGMENT

The author would like to thank Dan Scheiman, Paula Heimann, Toni Kapucinski, Tim Ubienski, Rich Martin, Bill Brown, Susan Puleo, and Wayne Jennings at NASA-Glenn Research Center (GRC) for technical supports, industrial collaborator MERSEN, New Product Development, Rochester, NY for bus bar prototype development, and the Center for High Performance Power Electronics (CHPPE, Prof. Jin Wang), Ohio State University, Columbus, OH for PD testing support. Furthermore, Maricela Lizcano and Azlin Biaggi-Labiosa, GRC as a project lead and manager, respectively, and the rest of project team are acknowledged for their supports.

REFERENCES

[1] E. E. Shin, D. A. Scheiman, and M. Lizcano, "Lightweight, Durable, and Multifunctional Electrical Insulation Material Systems for High Voltage Applications," Proceedings of the AIAA/IEEE Electric Aircraft Technologies Symposium (EATS), 2018 Joint Propulsion Conference, 9 - 13 July, 2018, Cincinnati, OH. 2018. AIAA Propulsion and Energy Forum (AIAA 2018-5013). https://doi.org/10.2514/6.2018-5013

[2] M. Lizcano, T. Williams, E. Shin, D. Santiago, B. Nguyen, "Challenges in High Voltage Aerospace Electrical Insulation in Extreme Environments," Materials 2022, 15(22), 8121; https://doi.org/10.3390/ma15228121 (registering DOI), Multidisciplinary Digital Publishing Institute (MDPI), 16 November 2022.

[3] I. Christou, "Optimisation of High Voltage Electrical Systems for Aerospace Applications," A Ph.D. thesis submitted to the university of manchester, Scool of Electrical and Electronic Engineering, 2011. https://research.manchester.ac.uk/files/54509388/FULL_TEXT.PDF

[4] E. E. Shin, "Development of High Voltage Micro-Multilayer Multifunctional Electrical Insulation (MMEI) System," Proceedings of the AIAA/IEEE Electric Aircraft Technologies Symposium (EATS), 22 -

24 August 2019, Indianapolis, IN. 2019 AIAA/IEEE Electric Aircraft Technologies Symposium. AIAA Propulsion and Energy Forum. (AIAA 2019-4511). https://doi.org/10.2514/6.2019-4511

[5] E. E. Shin, "Progresses in Developing Micro-Multilayer Multifunctional Electrical Insulation (MMEI) System for High Voltage Applications," Proceedings of the American Association for Advances in Functional Materials (AAAFM)-UCLA International Conference, 18 - 20 August 2021, Los Angeles, CA

[6] E. E. Shin, "High Performance Multilayer Insulation Composite For High Voltage Applications," United States Patent (U.S. Pat.) No. 10,546,666, January 28, 2020.

[7] NASA. Spacecraft High-Voltage Paschen and Coroana Design Handbook (NASA-HDBK-4007), 2016.

[8] T. Rahman, S. Amin, H. Shaukat, S. S. Haroon, I. A. Sajjad, and M. Awais, " Effect of nano filler concentration on leakage current and partial discharge properties of zepoxy nano composites," SN Applied Sciences (2019) 1:1218 | https://doi.org/10.1007/s42452-019-1227-4

[9] C.Richardson, "Compounding of Semiconductives for High Voltage Cables," Jicable '07, http://www.jicable.org/2007/Actes/Session_C51/JIC07_C512.pdf

[10] Y. Wei, W. Han, G. Li, Q. Lei, M. Fu, C. Hao, and G. Zhang, "Research progress of semiconductive shielding layer of HVDC cable," High Volt., 2020, Vol. 5 Iss. 1, pp. 1-6. https://doi.org/10.1049/hve.2019.0069

[11] T. Wang, X. Li, M. Liu, G. Li, W. Xiao, S. Chen, C. Hao, Y. Wei, M. Fu and Q. Lei, "Influence of charge emission behaviors of semi-conductive shielding layer on charge accumulation properties of insulation layer for HVDC cable," Mater. Res. Express 7, 2020, 125302. https://doi.org/10.1088/2053-1591/abcf7b

[12] H.-J. Choi, M. S. Kim, D. Ahn, S. Y. Yeo and S. Lee, "Electrical percolation threshold of carbon black in a polymer matrix and its application to antistatic fibre," Scientific Reports, 2019 9:6338. https://doi.org/10.1038/s41598-019-42495-1

[13] D. Pantea, H. Darmstadt, S. Kaliaguine, C. Roy, "Electrical conductivity of conductive carbon blacks: influence of surface chemistry and topology," Applied Surface Science vol. 217, 2003, pp. 181–193. https://doi.org/10.1016/S0169-4332(03)00550-6

[14] K.-Y. Lee, J.-C. Nam, D.-H. Park, D.-H. Park, "Electrical and Thermal Properties of Semiconductive Shield for 154KV Power Cable," Proceedings of 2005 lntemational Symposium on Electrical Insulating Materials, June 5-9, 2004, Kitakyushu, Japan